Inorg. Chem. **2009**, *48*, 3529−3534

Inorganic Chemistry
Article

Crystal and Molecular Structure of Manganese(II) Lapacholate, a Novel Polymeric Species Undergoing Temperature-Reversible Metal to Ligand Electron Transfer

Francesco Caruso,*,† Miguel A. Martínez,‡ Miriam Rossi,§ Alexander Goldberg,|| M. Elizabeth Chacón Villalba,⊥ and Pedro J. Aymonino⊥,#

Istituto di Chimica Biomolecolare, Consiglio Nazionale delle Ricerche (CNR), c/o Università di Roma"La Sapienza" Vecchio Istituto Chimico, P.le Aldo Moro 5, 00185 Rome, Italy, Facultad de Química, Bioquímica y Farmacia, Universidad Nacional de Tucumán, Tucumán, Argentina, Vassar College, Department of Chemistry, Box 484, Poughkeepsie, New York 12604-0484, Accelrys Inc., 10188 Telesis Court, Suite 100, San Diego, California 92121, and CEQUINOR (Centro de Química Inorgánica), CONICET, Facultad de Ciencias Exactas, Universidad Nacional de La Plata, Argentina

Received August 9, 2008

Lapachol (2-hydroxy-3-(3-methyl-2-butenyl)-1,4-naphtoquinone) (HLap, $C_{15}H_{14}O_3$) reacts with Mn^{2+} producing a novel polymeric complex with formula: $[Mn(Lap)_2]_n$. Two ligands chelate the metal through their *ortho* oxygen (O1, O2) moiety while two *para* oxygens, from other Lap ligands, complete the octahedral coordination sphere. Thus far, all reported Lap metal complexes are mononuclear, lack the metal-*trans*-quinonic (*para*) oxygen binding and have Lap as a bidentate ligand. Synthesis, X-ray diffraction, IR, and UV−visible spectroscopic properties, thermogravimetric analysis, and differential thermal analysis of this complex are reported along with a density functional theory study describing electron transfer from the Mn to the Lap ligand at low temperature. X-ray structure determinations at 125, 197, and 300 K describe the progressive trend of a Mn contribution to the Mn−O1 bond length as a function of *T*. The Mn−O1 bond distance increases with temperature and may be therefore associated with a semiquinonate action at low *T* by the carbonyl O1 donor (and corresponding to Mn^{III}). It transforms to a more classical coordinative bond at room *T* and stabilizes a Mn^{II} species; this is a reversible phenomenon involving Mn^{II}−Mn^{III} oxidation states.

Introduction

Lapachol, Scheme 1, is a natural product extracted from the wood of lapacho (*Tabebuia avellanedeae*) trees and other tropical plants. Lapacho grows in the rain forests of Argentina, Paraguay, Brazil, and other South American countries. A tea extract from the inner bark of the Lapacho tree has been used as a folk remedy against many diseases in South America since the time of the Incas. Growing interest in "natural" medicines has spread the use of lapacho tea to North-America and Europe. Lapachol is used against Chagas' disease and as an antineoplastic agent,[1] although other studies with laboratory mice show that lapachol promotes the formation of cancer.[2] Antimetastatic action of lapachol on B16 melanoma, at low dosage (5−20 mg/kg), is observed through an unknown mechanism whereas a high

Scheme 1. Lapachol, Including C Labeling Used in the X-ray Structure of $[Mn(Lap)_2]_n$

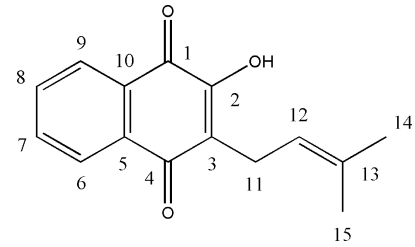

* To whom correspondence should be addressed. E-mail: caruso@vassar.edu.
† Consiglio Nazionale delle Ricerche.
‡ Universidad Nacional de Tucumán.
§ Vassar College.
|| Accelrys Inc.
⊥ Universidad Nacional de La Plata.
Deceased March 2008.

(1) Rao, K. V.; Mc Bride, T. J.; Olenson, J. J. *Cancer Res.* **1968**, *28*, 1952.

10.1021/ic8015194 CCC: $40.75
Published on Web 03/12/2009

toxic dose of lapachol promotes metastasis by inducing a hypercoagulable state as a result of vitamin K-dependent pathway inhibition.[3] Lapachol patents having medical applications have been increasing; there were 13 patents in 2008 alone.[4] Lapachol use is known to decrease blood coagulation in humans.[5]

Coordination complexes may slow the delivery of lapachol and so potentially be able to modulate and/or improve its therapeutic activity. Previously, we reported the complexes dilapacholatediethanolzinc(II), dilapacholateaqua(dimethylformamide)cobalt(II), and dilapacholateaqua(dimethylformamide)zinc(II);[6,7] all are neutral pseudo-octahedral complexes with two bidentate lapacholate anions binding the metal through their *ortho* oxygens (O1, O2), Scheme 1. They can be located either at the equatorial planes of the octahedron in *trans* positions[6] or one in the equatorial plane and the other in a meridian plane.[7] The remaining two octahedral sites are occupied by two non-lapachol ligands. Notably, as far as we know, all reported complexes of lapacholate are mononuclear (see refs 6−9 and refs therein).

While synthesizing other complexes of lapacholate and related ligands, we surprisingly found that the product obtained for the manganese(II) lapacholate complex, with dimethylformamide (DMF) completing the coordination sphere, contained only lapacholate in correspondence with the empirical formula $Mn(Lap)_2$. The temperature dependence on the molecular structure of this product was studied using results from single crystal X-ray diffraction studies taken at three different temperatures. It is a polymer in which lapachol acts as a tridentate ligand, with the two adjacent oxygen atoms (O1, O2) chelating the metal and the remaining *trans*-quinonic oxygen bound to a different metal center. We also describe the IR and UV−visible spectra, TGA and DTA behavior, and a DFT study of this novel species.

Experimental Methods

Synthesis and Chemical Characterization. Bis-(2-hydroxy-3-(3-methyl-2-butenyl)-1,4-naphtoquinonate)manganese(II), $[Mn(Lap)_2]_n$: 0.25 g of anhydrous manganese(II) acetate was dissolved in 20 mL of anhydrous dimethylformamide (DMF) and kept in a water bath at 50−60 °C. To it was added a solution of 0.5 g of lapachol in 20 mL of DMF, heated also to 50−60 °C; the resulting solution was filtered and left for 2 months. The obtained prismatic, dark red-brown crystals were separated by filtration, washed with acetone and dried. Later, it was determined that the polymer also forms in ethanol. Anal. Calcd for $C_{30}H_{26}MnO_6$: C, 67.04; H, 4.84. Found C, 66.90; H, 5.00, MP > 300 °C. The sample included in a KBr disk was explored between 4000 and 400 cm^{-1} using a Bruker IFS 66 spectrophotometer. Determinations of thermogravimetric analysis and differential thermal analysis (TGA-DTA) were made between room temperature and 500 °C with a Rigaku Thermal Analyzer under flowing oxygen at 50 mL/minute and heating rate 10 °C/minute. Electronic spectra were obtained with a Hewlett-Packard 845 2A Diode Array Spectrophotometer, as a solid and in DMF solution. A Bruker Apex-2 diffractometer was used with Mo Kα graphite-monochromatized radiation to collect data on a suitable crystal at several temperatures, see Table 1. The structure was solved and refined with ShelX.[10] Hydrogen atoms were calculated at idealized positions. The theoretical study involved calculations using software programs from Accelrys. Density functional theory (DFT) code DMol3 was applied to calculate energies, see below, and graphical displays were generated with Materials Studio Visualizer.[11] We employed Double Numerical Polarized (DNP) basis set that includes all the occupied atomic orbitals plus a second set of valence atomic orbitals plus polarized d-valence orbitals.[12] Correlation generalized gradient approximation (GGA) was applied in the manner suggested by Perdew−Burke−Ernzerhof (PBE).[13] Spin unrestricted approach was exploited with all electrons being considered explicitly. The real space cutoff of 5 Å was imposed for numerical integration of the Hamiltonian matrix elements. The self-consistent-field convergence criterion was set to the root-mean-square change in the electronic density to be less than 10^{-6} electron/Å^3. The convergence criteria applied during geometry optimization were 2.72×10^{-4} eV for energy and 0.054 eV/ Å for force. Calculations were performed using X-ray coordinates of the title compound for a mononuclear $Mn(Lap)_2$ complex model. The two ligands bound to Mn through O3b and O3c (Figure 2b) in the polymer species were replaced by modified lapachols having an H bound to O1b and O1c to allow neutral charge conservation. In addition, the dimethylethylene moiety, C11−C15, was replaced by a hydrogen atom; this is justified by the fact that the IR bands associated with C11−C15 are not affected upon metal coordination in the related IR spectra (deposited). Therefore, the model is $(Lap')_2Mn(HLap')_2$ where Lap′ differs from Lap in that the dimethylethylene moiety is missing. Energy and deformation density

Table 1. Crystallographic Data of $[Mn(Lap)_2]_n$ at 300 K

chemical formula	$C_{30}H_{26}MnO_6$
fw	537.47
crystal system	tetragonal
space group	$P4_12_12$
a, Å	13.3505(4)
b, Å	13.3505(4)
c, Å	14.7128(4)
V, Å^3	2622.3(1)
Z	4
crystal size, mm^3	0.46 × 0.30 × 0.15
δ, g/cm^3	1.361
μ, cm^{-1}	0.545
reflns [$I > 2\sigma(I)$]	3211
refined params	169
R (Rw)	0.0275 (0.0753)

(2) de Sandoval, N. A.; Rodríguez, C. P.; de Martinez, N. R. *Acta Physiol. Pharmacol. Ther. Latinoam.* **1996**, *46*, 257.
(3) Maeda, M.; Murakami, M.; Takegami, T.; Ota, T. *Toxicol. Appl. Pharmacol.* **2008**, *229*, 232.
(4) *Scifinder*, version 2009; Chemical Abstracts Service: Columbus, OH, 2009.
(5) Block, J.; Serpick, A. A.; Miller, W.; Wiernick, P. H. *Cancer Chemother, Rep. Part 2* **1974**, *4*, 27.
(6) Martinez, M. A.; de Jiménez, C. L.; Castellano, E. E.; Piro, O. E.; Aymonino, P. J. *J. Coord. Chem.* **2003**, *56*, 803.
(7) Martinez, M. A.; De Jiménez, C. L.; Castellano, E. E.; Piro, O. E.; Aymonino, P. J. *J. Argent. Chem. Soc.* **2005**, *93*, 183.
(8) Hernández-Molina, R.; Kalinina, I.; Esparza, P.; Sokolov, M.; González-Platas, J.; Estévez-Braun, A.; Pérez-Sacau, E. *Polyhedron* **2007**, *26*, 4360.
(9) De Oliveira, E. H.; Medeiros, G. E. A.; Peppe, C.; Brown, M. A.; Tuck, D. G. *Can. J. Chem.* **1997**, *75*, 499.
(10) Sheldrick, G. M. *SHELXTL, An Integrated System for Solving, Refining, and Displaying Crystal Structures from Diffraction Data*; University of Göttingen: Göttingen, Germany, 1981.
(11) *Materials Studio Visualizer*; Accelrys Software Inc.: 10188 Telesis Court, Suite 100, San Diego, CA 92121, U.S.A.
(12) Perdew, J. P.; Chevary, J. A.; Vosko, S. H.; Jackson, K. A.; Pederson, M. R.; Singh, D. J.; Fiolhais, C. *Phys. Rev. B: Cond. Mat. Mater. Phys.* **1992**, *46*, 6671.
(13) Becke, A. D. *Phys. Rev.* **1988**, *A38*, 3098.

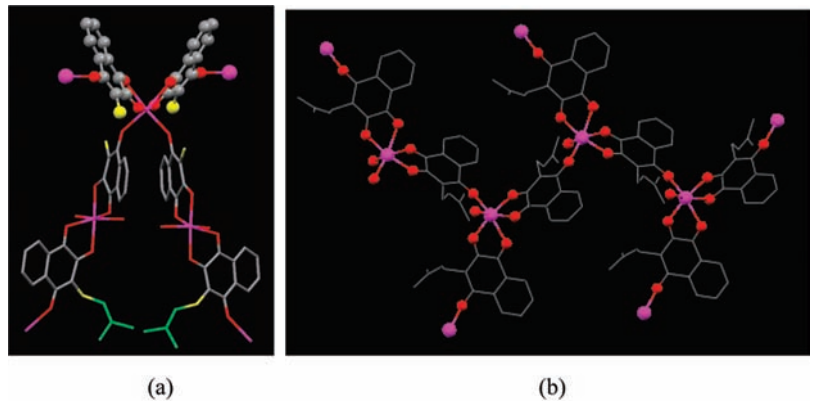

Figure 1. (a) Display of the polymeric complex $[Mn(Lap)_2]_n$ showing the complete coordination sphere for the top-center metal; Mn purple, O red, C gray, except green dimethylethylene group C12, C13, C14, and C15, omitted in the upper part, and its attached yellow C11; H omitted. (b) Four Mn units from the extended structure of $[Mn(Lap)_2]_n$ (Mn purple, O red, C gray, H omitted).

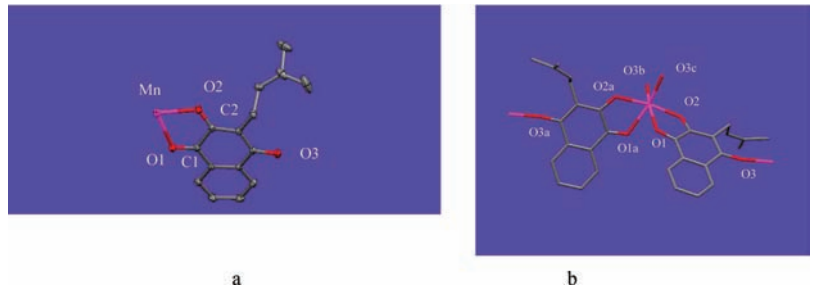

Figure 2. (a) Crystallographic asymmetric unit of $[Mn(Lap)_2]_n$ showing displacement parameters. (b) Coordination around Mn(II); the crystallographic 2-fold axis, almost vertical in this view, bisects the O3b−Mn−O3c angle.

of this model were calculated for structures derived from the X-ray study at 125 K and at 300 K.

Results and Discussion

X-ray Diffraction. Figure 1 displays the polymeric features of the title compound from data taken at room temperature, Figure 2a shows the asymmetric unit and Figure 2b depicts the coordination sphere. Atom labeling of lapacholate is consistent with that of Scheme 1, but the O−4 atom was labeled O3 in the crystal structure. In the coordination sphere, atoms belonging to the second lapacholate are labeled as "a", and the *para*-oxygen O3 are named O3b and O3c, Figure 2b. A distorted octahedral coordination of Mn(II) is seen as the *trans* angles [168.96(6)° (O2−Mn−O2a), 164.32(4)° (O1−Mn−O3b and O1a−Mn−O3c)] are markedly different from 180°, Table 2; this is probably due to constraints imposed by the lapacholate bite angle [73.30(4)°]. For the least-squares equatorial plane defined by O1, O2, O2a, and O3b the metal is located 0.15 Å out of plane toward O3c. The central part of Figure 1a also shows the short stacking distance between the lapacholate ligands, bonded through O3 atoms to the same Mn nucleus; both naphthalene rings are almost parallel forming an angle of 8.6°; the shortest separation is for C4b−C5c = 3.46 Å, and compares well to the stacking distance in graphite (3.37 Å), suggesting a π-π interaction.

For C−O bond analysis, C1−O1 has the shortest bond length, 1.2241(17) Å, suggesting a stronger double bond character and weaker donation to the metal, compared with C2−O2 [1.2732(18) Å] and C4−O3 [1.2556(16) Å]. This is consistent with the fact that Mn−O1 [2.3208(12)] is longer than Mn−O2 [2.1060(10)] and Mn−O3 [2.1131(11) Å].

Table 2. Selected Bond Lengths (Å) and Angles (deg) in $[Mn(Lap)_2]_n$

distances		angles	
Mn−O1	2.3209(12)	O1−Mn−O2	73.30(4)
Mn−O2	2.1061(10)	O1−Mn−O3b	164.32(4)
Mn−O3b	2.1131(11)	O1−Mn−O1a	79.17(6)
Mn1−O3c	2.1131(11)	O1−Mn−O2a	97.99(4)
O1−C1	1.2241(17)	O1−Mn−O3c	95.35(4)
O2−C2	1.2732(18)	O1a−Mn−O3c	164.32(4)
O3−C4	1.2556(16)	O2−Mn−O3b	93.15(5)
C1−C2	1.512(2)	O2−Mn−O1a	97.99(4)
C1−C10	1.472(2)	O2−Mn−O2a	168.96(6)
C2−C3	1.385(2)	O2−Mn−O3c	94.41(5)
C3−C4	1.416(2)	O3b−Mn−O1a	95.35(4)
C4−C5	1.497(2)	O3b−Mn−O2a	94.41(5)
C5−C10	1.399(2)	O3b−Mn−O3c	93.51(6)
C6−C7	1.388(3)	C1−O1−Mn	112.7(1)
C7−C8	1.377(3)	C2−O2−Mn	119.7(1)
C8−C9	1.379(3)	C4b−O3b−Mn	146.8(1)
C9−C10	1.389(2)	C4c−O3c−Mn	146.8(1)

The title compound can be compared to $[Zn(Lap)_2(EtOH)_2]$, where the lapacholate ligands are *trans* to each other in inverted equatorial positions as the Zn atoms are located at an inversion center and the remaining two octahedral positions are occupied by O(ethanol) atoms that form H-bonds to O3 atoms from neighboring lapacholate units.[6] The planar $Zn(Lap)_2$ units are stacked [3.08(3) Å] and have the lapacholate ligands above and below, similar to the nearly antiparallel lapacholates in the title compound. The sequence of C−O bond lengths in $[Zn(Lap)_2(EtOH)_2]$ is as follows: C1−O1 [1.226(3) Å] < C4−O3 [1.243(3) Å] < C2−O2 [1.279(3) Å], similar to the pattern shown in the title compound. Also, the Zn−O bond distances in

Table 3. Selected Structural Data of $[Mn(Lap)_2]_n$ at Different Temperature Data Collection

T	Mn−O1	Mn−O2	Mn−O3b	C1−O1	C2−O2	C4−O3	O1−Mn−O2
125 K	2.3117(9)	2.1042(7)	2.1114(8)	1.2304(12)	1.2733(13)	1.2572(12)	73.84(3)
197 K	2.316(1)	2.1037(9)	2.1115(9)	1.2298(14)	1.2736(15)	1.2565(14)	73.67(3)
300 K	2.321(1)	2.106(1)	2.113(1)	1.2241(17)	1.2732(18)	1.2556(16)	73.30(4)

$[Zn(Lap)_2(EtOH)_2]$ (Zn−O1 = 2.183(2) and Zn−O2 = 1.991(2) Å), follow the same pattern as seen in the Mn complex, but the metal−O1 bond length is markedly longer in the title compound.

Comparison of $[Mn(Lap)_2]_n$ to Mn-quinone compounds is of interest as Mn is a cofactor associated with catalysis of oxygen evolution in photosystem II[14] and quinones are present in choloroplasts and also thought to be involved in photosystem II.[15] Pierpont, et al. discussed valence tautomerism and showed that in neutral $MnL(benzoquinone)_2$ complexes, L = diamine or bis-amines, the metal can release electronic charge to the aromatic system. The largest amount of electron transfer makes the benzoquinone ligands behave as catecholates stabilizing Mn^{IV}, that is, two electrons are transferred to each quinone. The weakest amount of electron transfer is associated with Mn^{II} and benzoquinone behaving as a simple coordinative ligand; intermediate electron transfer is associated with Mn^{III} and benzoquinone behaving as a semiquinone radical.[16] As far as we know, for 1:2 Mn/ligand ratio, the title compound is unique because there are no additional ligands completing the coordination sphere of Mn, and so a straightforward comparison of electron transfer properties with previous Mn-quinone compounds may be speculative, especially since the two O(carbonyl) atoms (both O3 belonging to two additional lapachol donors) also may be involved in charge transfer.

From the literature, a comparison can be made with Mn(3,6-di-*tert*-butyl-1,2-benzoquinone)$_3$. Its MnO_6 coordination sphere is similar to the title compound, and the ligand is also an aromatic ketone. Interestingly, this complex shows a mixed $Mn^{III}-Mn^{IV}$ species because it is associated with features of cathecholic-Mn^{IV} behavior (Mn−O bond length about 1.90 Å) along with semiquinonate Mn^{III} longer bonds.[16] Indeed, it has been shown that Mn−O bond lengths are the shortest for Mn^{IV}, the longest for Mn^{II}, and intermediate for Mn^{III}.[16] We can assume that our complex is not a Mn^{IV} species as our Mn−O bond lengths are longer than 1.90 Å. Mn^{III} complexes show Jahn−Teller elongation of axial bonds or display the geometry of a prismatic triangular coordination polyhedron.[16] Since these features are absent in the title compound, a Mn^{II} species seems to be the only logical possibility. However, complexes described as mixed electronic Mn species show the Mn electronic state may be modified as a function of temperature so that a mixed $Mn^{IV}-Mn^{III}$ species evolves to Mn^{III} upon heating or, alternatively and probably more in agreement with the title compound, a $Mn^{III}-Mn^{II}$ mixed species can evolve toward Mn^{II}. Therefore, we decided to collect X-ray diffraction data at 125 K for the title compound and check for evidence of Mn^{III} existence, see Table 3.

At 125 K the Mn−O bond lengths, Mn−O1 2.3117(9) Å, Mn−O2 2.1042(7) Å, and Mn−O3 2.1114(8) Å, are shorter than those at room temperature (300 K) but only Mn−O1 differs significantly (using ESD's) among the three data sets. This pattern may be therefore associated with a semiquinonate action at low *T* for the O1 donor that transforms to a more classical coordinative bond at room *T* stabilizing a Mn^{II} species. In the coordination polyhedron Mn−O2 has the shortest bond length, which is consistent with the lapacholate anionic character as in the 300 K structure. The influence of both "formal" carbonyls C1═O1 and C4═O3 on the metal is markedly different as shown by Mn−O1 [2.3117(9) Å] and Mn−O3 [2.1114(8) Å] bond lengths, which differ 223σ, and demonstrate a greater involvement of O3 as a donor. However, of these two carbonyls, only O1 contributes to further donation at low temperature by shortening the Mn−O1 bond length, Table 3.

Additional information from the 125 K data collection shows that C2−O2 [1.2733(13) Å] is significantly longer than O1−C1 [1.2304(12) Å] and C4−O3 [1.2572(12) Å], 33σ and 13σ different, respectively, and so confirming the C2−O2 single bond character. This agrees with Mn−O2 having the shortest Mn−O bond in the coordination sphere because of the lapacholate anionic character as mentioned earlier. C1−O1 is shorter than C4−O3 (by 14σ) and is consistent with a Mn contribution to the Mn−O1 bond at 125 K. Furthermore, comparing C1−O1 bond lengths at 125 K [1.2304(12) Å] and 300 K [1.2241(17) Å] shows that they are significantly different, as their range of variation within 3σ differ [1.2298−1.2440] Å and [1.2190−1.2292] Å, respectively.

An additional data collection at 197 K shows intermediate bond distance values, also tabulated in Table 3, and confirming the progressive trend of a Mn contribution to Mn−O1 bond length as a function of *T*.

TGA-DTA. In addition to their specific interest, the TGA results confirm the compound formula. Figure 3 reproduces the result of a TGA run, which shows that the oxidation reaction begins at about 311 °C and ends at about 420 °C and that it is produced in steps, possibly because it begins with the oxidation of the butenyl groups. The total ΔMW is 84.92%, while the expected value for the formation of the Mn_2O_3 is 85.42%.

IR Spectrum. Supporting Information, Figure S1, depicts the FTIR spectrum of $[Mn(Lap)_2]_n$ in KBr. The bands located between 3100 and 2850 cm^{-1} are assigned to aliphatic and aromatic C−H stretching. The characteristic ν(C═O) stretch-

(14) (a) Mullins, C. S.; Pecoraro, V. L. *Coord. Chem. Rev.* **2008**, *252*, 416. (b) Livorness, J.; Smith, T. D. *Struct. Bonding (Berlin)* **1982**, *48*, 1.
(15) (a) Knaff, D. B.; Malkin, R.; Myron, J. C.; Stoller, M. *Biochem. Biophys. Acta* **1977**, *459*, 402. (b) van Gorkon, J. *Biochem. Biophys. Acta* **1974**, *347*, 439.
(16) Attia, A. S.; Pierpont, C. G. *Inorg. Chem.* **1998**, *37*, 3051.

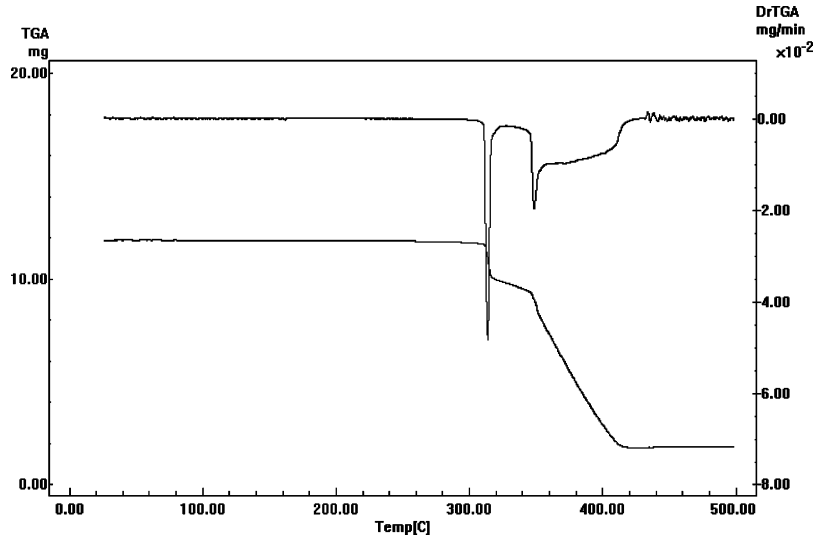

Figure 3. TGA and DTGA of $[Mn(Lap)_2]_n$ under oxygen flow.

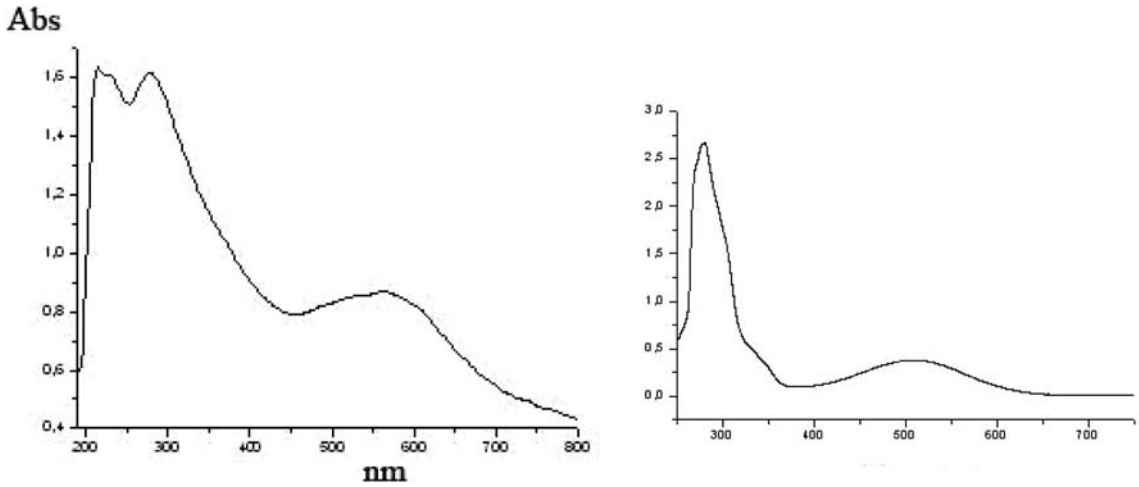

Figure 4. UV−vis spectrum of $[Mn(Lap)_2]_n$ as a solid included in KBr (left) and in DMF solution (right).

ing bands, found at 1660 and 1639 cm^{-1} in free Lapachol,[17] are shifted to lower frequencies in the complex (1646 and 1583 cm^{-1}) also observed in other lapacholate complexes.[5,7,17−20] The band located at 3351 cm^{-1} in lapachol,[17] assigned to OH, disappears upon coordination, as expected. A number of new bands are seen after complex formation, most notably those found at 1530 (sh), 1505 (vs), and 1475 (s) cm^{-1}, but interestingly, the characteristic 1369 cm^{-1} band of lapachol assigned to CH-scissors mode of the lateral chain holds the same position and intensity in the complex. Besides the 724 cm^{-1} band of lapachol, assigned to an out of the plane ring mode, is shifted to 735 cm^{-1} in the complex.

In general, and as shown by previous theoretical calculations,[17] a definite assignment in the spectral range between 1400 and 700 cm^{-1} is rather difficult because of important vibrational mixing. Finally, new bands located below 500 cm^{-1} may be related to metal-to-ligand vibrations; they are found at 460, 488, 440, and 425 cm^{-1}, the first of medium intensity and the remaining ones of weak intensity.

UV−vis Spectra. The UV−visible spectra of the Mn complex in DMF solution and the solid are shown in Figure 4. The former is similar to that of $[Zn(Lap)_2(EtOH)_2]$ in ethanol[6] for frequencies higher than 350 nm. The crystals of the title compound are dark red-brown, in marked contrast with lapachol and its sodium salt which are yellow. The broad and relatively intense absorption band located at 510 nm in the spectrum of the solution, and at 550 nm in the solid, is associated with the color. In literature references,[16] near-infrared electronic spectra bands in the solid (2200−2660 nm) have been associated with valence tautomerism. Therefore, such an assignment for the 550 nm band in the solid is not consistent with this interpretation, and so an exploration of this near IR spectra will be performed in the near future. The intense band located at 282 nm and the shoulders at 332 and 306 nm could be assigned to $\pi \rightarrow \pi^*$ transitions in the aromatic rings.[6,7]

Theoretical Calculations. To analyze the potential electronic transfer from Mn to ligand and vice versa at various

(17) Farfan, R.; Molina, J.; Ottavianelli, E.; Espindola, J. *Inf. Tecnol.* **2006**, *17*, 63.
(18) Dufresne, A.; De Lima, C. G.; Knudsen, J.; Moreira, E. *J. Inorg. Nucl. Chem.* **1973**, *35*, 789.
(19) Khandagale, P.; Chikate, R.; Joshi, S. B.; Kulkarni, B. A. *J. Alloys Compd.* **2005**, *392*, 112.
(20) Garge, P.; Chikate, R.; Padhye, S.; Savariault, J.; de Loth, P.; Tuchages, J. *Inorg. Chem.* **1990**, *29*, 3315.

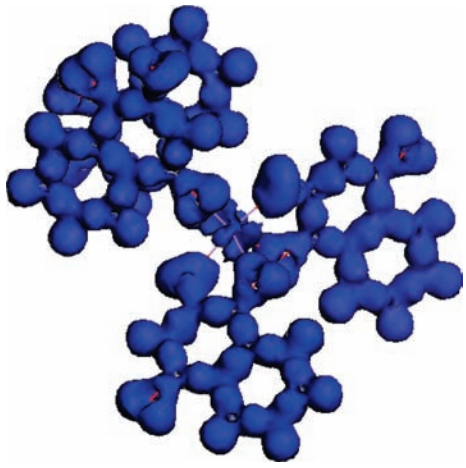

Figure 5. Total deformation electron density at 0.03 e/Å^3 of the lapacholate model from low temperature (125 K) structural data.

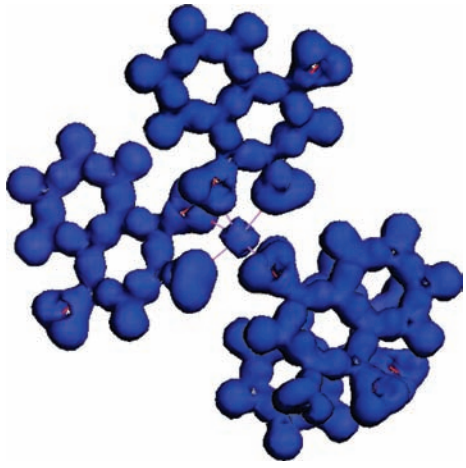

Figure 6. Total deformation electron density at 0.03 e/Å^3 of the Mn lapacholate model from room temperature (300 K) structural data.

temperatures, we compare deformation electron density for a Mn lapacholate model at two different temperatures, 125 K and 300 K, using coordinates from the corresponding data collections of the title compound. These models are mononuclear arrangements to simplify calculations where only energy is optimized, and so the coordinates of the main atoms are kept as experimentally determined. Figure 5 and 6 show the deformation electron density surface at 0.03 e/Å^3, which is calculated as the difference between the total electron density of the entire molecule and the density of the isolated atoms; they include only a positive deformation density range. At 125 K, Figure 5, the charge density is distributed around the Mn atom and the ligand, suggesting electron density formation on both Mn atom and the ligand. Figure 6 depicts the same calculation for the 300 K structure showing electron density formation more concentrated around the Mn atom. This higher electron density on the metal atom is due to electron transfer from the ligand to the metal, consistent with a d^5 Mn^{II} state, and so the low temperature structure is associated at least with a partial Mn^{III} contribution. These results agree with the X-ray structural features showing variation of Mn−O1 bond length, and so a shift in oxidation state from Mn^{III} to Mn^{II} is associated with increasing temperature.

Conclusions

In spite of the high coordination capacity of DMF which stabilizes many transition metal complexes of lapacholate,[6,7] the crystalline product obtained from a solution of that potential ligand with Mn(II) is shown by single crystal X-ray diffraction to be a novel polymer, $[Mn(Lap)_2]_n$. The lapacholate anion acts as a tridentate ligand while all previously described lapacholate complexes are mononuclear of general formula $M(Lap)_2X_2$, in which the anion is exclusively bidentate. The 3-methyl-2-butenyl IR band, labeled C11−C15 in the crystal structure, is not affected when lapachol is complexed to the Mn title compound. A DFT model of the title compound, based on corresponding X-ray coordinates, shows electron transfer from the Lap ligand to the metal with increasing temperature; it is associated with Mn^{III}−Mn^{II} variation and consistent with corresponding geometrical features as seen from diffraction studies at three different temperatures performed in this study.

Acknowledgment. Financial support from the Schools of Exact Sciences (U.N.L.P.) and Biochemistry, Chemistry, and Pharmacy (U.N.T.), and CEQUINOR-CONICET. M.E.C.V. thanks CICPBA for financial support.

Supporting Information Available: FTIR spectrum of $[Mn(Lap)_2]_n$ in KBr (Figure S1), IR frequencies of Lapachol (HLap) and $[Mn(Lap)_2]_n$ (Table S1), crystallographic CIF files of $[Mn(Lap)_2]_n$. This material is available free of charge via the Internet at http://pubs.acs.org.

IC8015194